AD-A096 229 TRACOR INC ROCKVILLE MD F/G 20/6
EXPERIMENTAL MEASUREMENTS OF THE RATE OF CHANGE OF THE INDEX-OF--ETC(U)
AUG 80 V PROVENZANO N00014-78-C-0886
UNCLASSIFIED TRACOR-T-81-RV-5031 NL

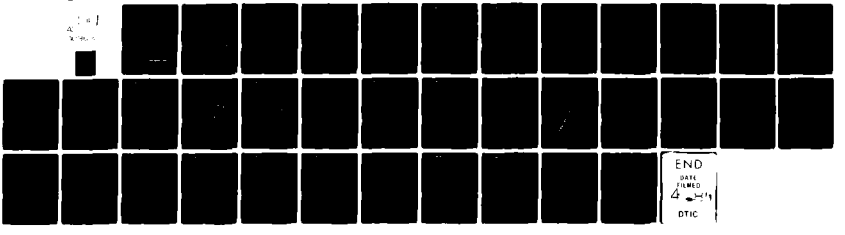

END
DATE FILMED
4-81
DTIC

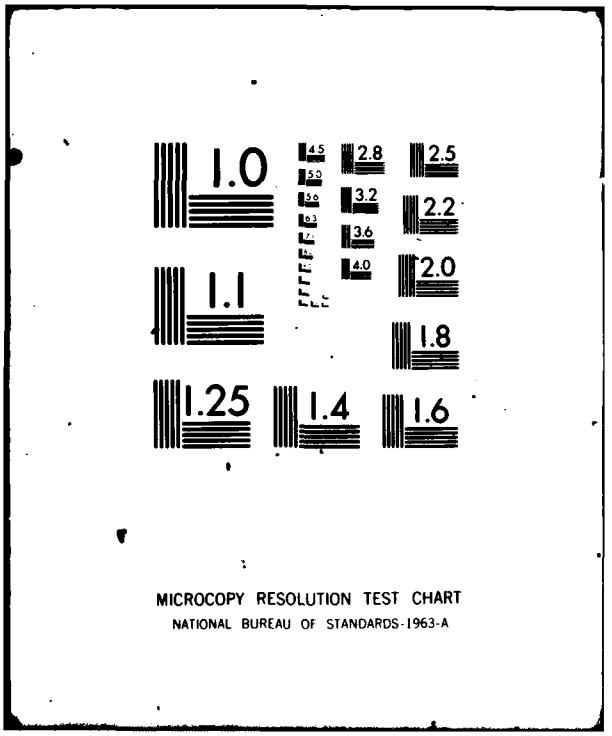
1.0
1.1
1.25
1.4
1.6
1.8
2.0
2.2
2.5
2.8
3.2
3.6
4.0
4.5
5.0
5.6
6.3
MICROCOPY RESOLUTION TEST CHART
NATIONAL BUREAU OF STANDARDS-1963-A

Contract No.: N00014-78-C-0886
Document No.: T-81-RV-5031

FINAL REPORT

EXPERIMENTAL MEASUREMENTS OF THE RATE OF CHANGE OF THE INDEX-OF-REFRACTION OF OPTICAL FIBER MATERIALS WITH RESPECT TO TEMPERATURE AND PRESSURE

Submitted to:
Office of Naval Research
Department of the Navy
800 N. Quincy Street
Arlington, Virginia 22217

Attn: Dr. R. Pohanka, Code 471

22 August 1980

Tracor Applied Sciences

Tracor, Inc.
1601 Research Blvd.
Rockville, Maryland 20850
Telephone 301:279-4200

(15)

Contract No.: N00014-78-C-0886
Document No.: T-81-RV-5031

(14) TRACOR-T-81-RV-5031

(9) FINAL REPORT

(12) 37

(6) EXPERIMENTAL MEASUREMENTS OF THE RATE OF CHANGE OF THE INDEX-OF-REFRACTION OF OPTICAL FIBER MATERIALS WITH RESPECT TO TEMPERATURE AND PRESSURE.

(10) V. / Provenzano

Submitted to:
Office of Naval Research
Department of the Navy
800 N. Quincy Street
Arlington, Virginia 22217

Attn: Dr. R. Pohanka, Code 471

(11) 22 Aug 80

Approved by:

J. Guarnieri, Manager
Special Systems Branch

Prepared by:

V. Provenzano
Principal Scientist

TABLE OF CONTENTS

LIST OF ILLUSTRATIONS

TABLE OF CONTENTS (Continued)

LIST OF TABLES

1.0 SUMMARY

During the past year, Tracor, under contract for the Office of Naval Research (ONR), has been conducting optical measurements on fiber optical materials. These measurements were performed within the context of the Fiber Optic Sensor System (FOSS) program, relating to the development of the optical hydrophone and other optical sensors. The basic aim of the optical measurements was to characterize the elasto-optic properties of doped-silica glass samples as a function of dopant and dopant concentration. The relevant elasto-optic constants were the rate of change of the index of refraction with respect to temperature and pressure, the coefficient of thermal expansion, and the compressibility. The measurements were conducted on doped-silica samples furnished to Tracor by Corning Glass Works. To check the validity of the experimental results, two additional pure silica samples were included in the investigation.

Laser interferometry was employed for the optical measurements. For each glass sample, the experimental technique consisted of measuring two separate fringe rates from two sets of Fizeau fringes as either the temperature or the pressure on the sample was varied. The two sets of Fizeau fringes resulted from two interferometer arrangements. Water was used both as the thermal bath in the temperature measurements, and as the compressive fluid in the pressure measurements.

Inconsistencies, present in the literature concerning the optical parameters of water (the rate of change of the index of refraction with respect to temperature and pressure), produced large errors in the experimental results. These experimental errors were greatly reduced when the $\frac{dn}{dT}$ and $\frac{dn}{dp}$ of the glass samples were computed using independently measured index of refraction, expansion coefficient, α, and compressibility, k, and not using the optical parameters of water. Most of the remaining experimental uncertainty in the values of $\frac{dn}{dT}$ and $\frac{dn}{dp}$ was traced to large inhomogeneities present in the doped-silica samples, while the results on the two

pure silica samples fell within a few percent of the accepted literature values. Thus, the presence of large inhomogeneities in the doped-silica samples limit the usefulness of the experimental results.

Recommendations have been recently submitted through a Tracor proposal to the Office of Naval Research (ONR) and to the Naval Research Laboratory (NRL) for review and comments. In the proposal, it was recommended that the optical measurements be conducted on better quality glass samples, using experimental techniques that do not involve water.

2.0 INTRODUCTION

At the Naval Research Laboratory (NRL) major efforts are underway to develop the optical hydrophone and other optical sensors. These efforts are being supported by the Navy through the Fiber Optic Sensor System (FOSS) program. Of prime importance to these optical sensor developments is the characterization of the optical parameters in fiber optical materials. The relevant optical parameters for the above materials are the rate of change of index of refraction with respect to temperature and pressure, the elasto-optic constants, and the Pockels coefficients.

During the past year, Tracor, under ONR Contract No. N00014-78-C-0886, has been conducting optical measurements on doped-silica glass samples. The objectives of the optical measurements were to determine for each glass sample, the following quantities:

- The rate of change of the index of refractions with respect to temperature and pressure: $\frac{dn}{dT}$ and $\frac{dn}{dp}$.
- The coefficient of thermal expansion and compressibility: α and k.

The above quantities were measured on a group of 7 doped-silica samples provided to Tracor by Corning Glass Works, Corning, New York. The dopants were GeO_2, B_2O_3 and P_2O_5 with varying concentrations. Two additional fused-silica samples were included in the optical measurements to check the validity of the experimental results and establish base-line values for the above quantities. The experimental technique used for the optical measurements was laser interferometry. The technique will be described in the next section of this report. Following the description of the experimental technique, the results of the investigation will be presented and discussed. Finally, conclusions will be drawn and appropriate recommendations will be made.

3.0 FIZEAU INTERFEROMETRY

Two interferometer arrangements were employed to conduct the optical measurements on the doped-silica glass samples. For each glass sample, the interferometer arrangements allowed the determination of the rate of change of the index of refraction with respect to temperature, $\frac{dn}{dT}$, and the coefficient of thermal expansion, α, for the temperature measurements; and the rate of change of the index of refraction with respect to pressure, $\frac{dn}{dp}$, and the compressibility, k, for the pressure measurements. The interferometer arrangements produced two sets of Fizeau fringes by the interference of the beams reflected from the front and rear faces of the glass sample. As the temperature or the pressure was changed, the Fizeau fringes moved across the aperture as a result of the changing optical path length in the sample. From the measurement of two sets of fringe rates, $\frac{dn}{dT}$, α, $\frac{dn}{dp}$ and k were determined. In Sections 3.1 and 3.2 the pertinent theory concerning the interferometric technique and the corresponding experimental apparatus will be discussed in detail.

3.1 Theory

Figure 3-1 is a schematic diagram of the experimental arrangement used to obtain the first set of Fizeau fringes. The order number of interference fringes, N_1, produced by the interference of rays 1 and 2 when the monochromatic laser beam impinges upon the glass sample close to normal incident is given by:

$$N_1 = \frac{2nt}{\lambda}, \qquad (3\text{-}1)$$

where n is the index of refraction of the sample, t is the thickness and λ is the laser wavelength. Equation (1) relates the difference in the optical path length 2nt, between the reflected ray from the front surface and the reflected ray from the rear surface of the glass sample. Differentiating

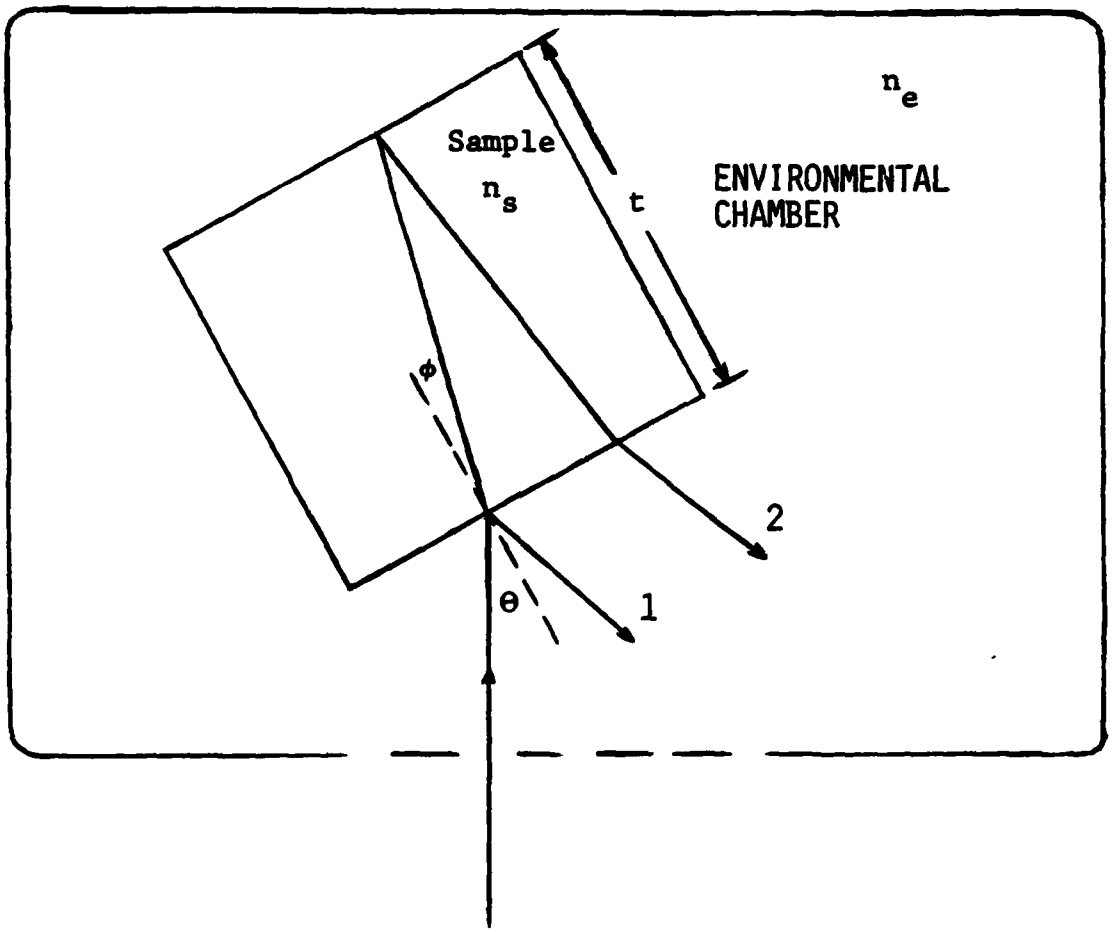

FIG. 3-1. Interferometer Arrangement for First Set of Fizeau Fringes.

Eq. (1) with respect to temperature, one gets the fringe rate for the first set of Fizeau fringes:

$$\frac{dN_1}{dT} = \frac{2}{\lambda}\left(n\frac{dt}{dT} + t\frac{dn}{dT}\right) = \frac{2t}{\lambda}\left(n\frac{1}{t}\frac{dt}{dT} + \frac{dn}{dT}\right) = \frac{2t}{\lambda}\left(n\alpha + \frac{dn}{dT}\right) \quad (3\text{-}2)$$

Equation (2) shows that the fringe rate with respect to temperature is due to changes both in length and in the refractive index of the sample. Since the changes in the index of refraction and in the length are coupled together in Eq. (2), the second interferometer arrangement shown schematically in Fig. 3-2, allows the independent determination of α the glass sample. Referring to Fig. 3-2, the fringe order number, N_2, for the second set of Fizeau fringes close to normal incident is given by:

$$N_2 = \frac{2n_e t}{\lambda}, \quad (3\text{-}3)$$

where n_e is the index of refraction of the environmental medium. The environmental medium was water both as the thermal bath for the temperature measurements, and as the compressive fluid for the pressure measurements. Differentiating Eq. (3) with respect to temperature one obtains:

$$\frac{dN_2}{dT} = \frac{2}{\lambda}\left(n_e\frac{dt}{dT} + t\frac{dn_e}{dT}\right) \quad (3\text{-}4)$$

where $\frac{dn_e}{dT}$ is the rate of change of the index of refraction of the water with respect to temperature. The values of α and $\frac{dn}{dT}$ of the glass sample are determined from the simultaneous solution Eqs. (2) and (4) and from the measurements of fringe rates in the two interferometer arrangements. That is:

$$\frac{dn}{dT} = \frac{n}{n_e}\frac{dn_e}{dT} + \frac{\lambda}{2t}\left(\frac{dN_1}{dT} - \frac{n}{n_e}\frac{dN_2}{dT}\right) \quad (3\text{-}5)$$

and

$$\alpha = \frac{1}{t}\frac{dt}{dT} = \frac{1}{n_e t}\left(\frac{\lambda}{2}\frac{dN_2}{dT} - t\frac{dn_e}{dT}\right) \quad (3\text{-}6)$$

Therefore, the fringe rates $\frac{dN_1}{dT}$ and $\frac{dN_2}{dT}$ are determined experimentally from the two interferometer arrangements; λ, n and t are known quantities, while

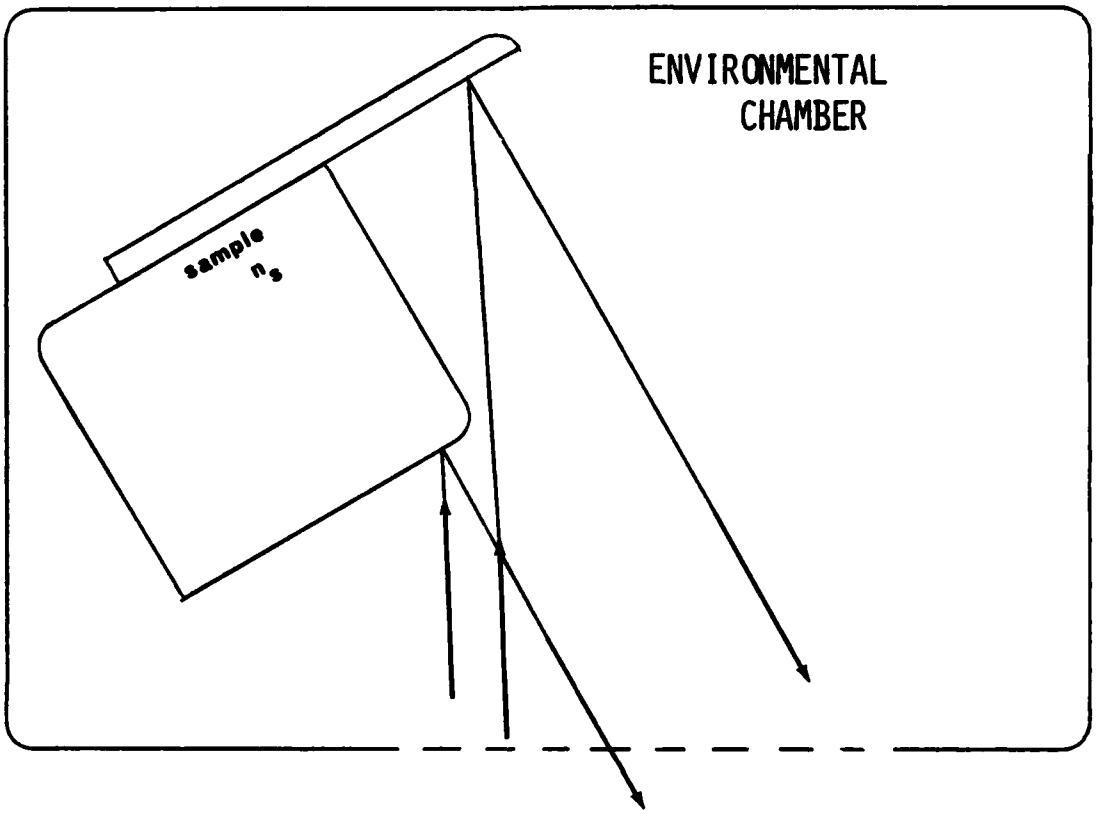

EXPERIMENTAL SET-UP #2

FIG. 3-2. Interferometer Arrangement for Second Set of Fizeau Fringes.

n_e, and $\frac{dn_e}{dT}$ are available in the literature. Similarly, the value of $\frac{dn}{dp}$ and k of the glass sample can be determined by measuring the fringe rates with respect to pressure. That is,

$$\frac{dn}{dp} = \frac{n}{n_e}\frac{dn_e}{dp} + \frac{\lambda}{2t}\left(\frac{dN_1}{dp} - \frac{n}{n_e}\frac{dN_2}{dp}\right) \text{ and} \tag{3-7}$$

$$k = \frac{3}{n_e t}\left(\frac{\lambda}{2}\frac{dN_2}{dp} - t\frac{dn_e}{dp}\right) \tag{3-8}$$

As in the temperature case, the value of $\frac{dn_e}{dp}$ for water should be easily found in the literature.

3.2 Experiment

The experimental apparatus used to produce the first set of Fizeau fringes both for the temperature and pressure measurements is presented in Fig. 3-3. The light source was a Spectra Physics Model 164 argon laser with 514.5 and 488 nm lines. A converging lens, whose focal point, was close to the rear face, directed the laser beam to the glass sample. The Fizeau fringe pattern was produced by the rear and front face reflections of the sample. The fringe motion, due to either temperature and pressure changes, was detected by a DC biased photo-darlington detector and graphically stored with a strip chart recorder; Linear Instruments, Model 255.

Figure 3-4 shows the experimental setup used to obtain the second set of Fizeau fringes. The interferometer arrangement is basically the same as that shown in Fig. 3-3, except that the fringe pattern in this case was produced by the interference of the beam reflected from the front face and the beam reflected from a small mirror attached to the rear face of the sample. Since the Fizeau fringes in this second arrangement were produced by the interference of light rays that were external to the glass sample, the fringe motion across the photo-detector as either the temperature or the

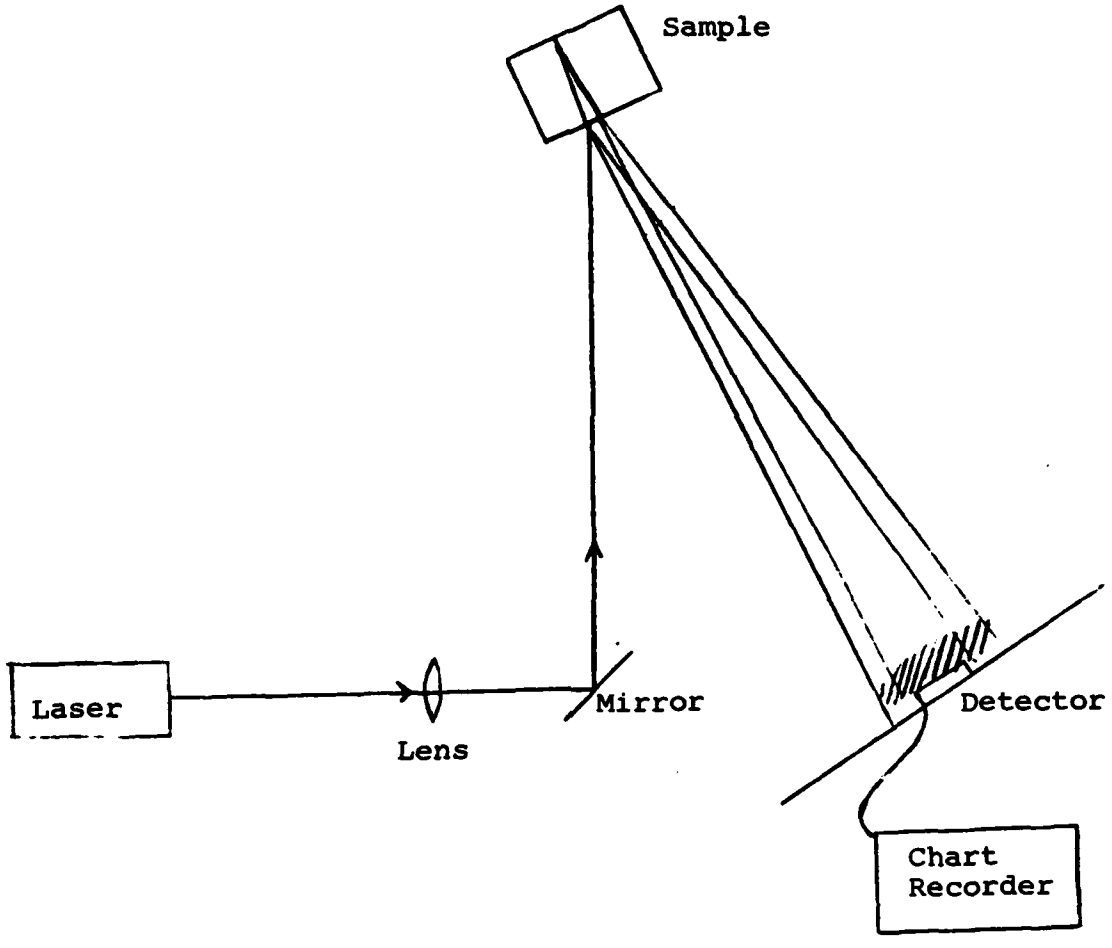

FIG. 3-3. Schematic of Experimental Apparatus for First Set of Fizeau Fringes.

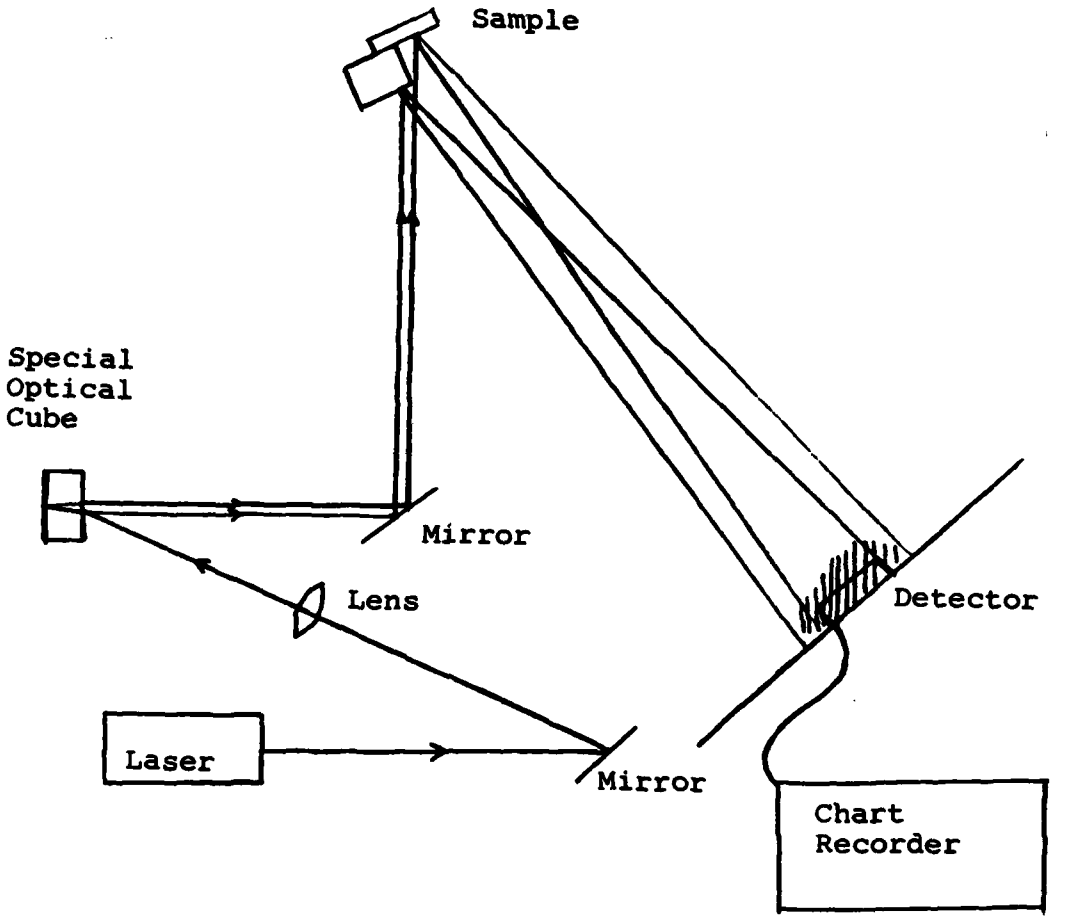

FIG. 3-4. Schematic of Experimental Apparatus for Second Set of Fizeau Fringes.

pressure was varied, resulted from changes in the thickness of the sample and from changes in the index of refraction of water. Thus, the fringe rates measured by the second interferometer arrangement allowed determination of dimensional changes in the glass sample provided that the rates of change of the index of refraction of water with respect to temperature and pressure were independently known. The dimensional changes and the changes in the index of refraction of the sample were coupled in the first set of Fizeau fringes.

The temperature bath used for the temperature measurements is shown in Fig. 3-5. The sample was suspended in the water by a metal positioning device which isolated it from the bottom of the tank. An immersion heater was used to raise the temperature of the bath, and when the bath temperature had reached about 80°C, the heater was turned off and the water was allowed to cool. The temperature of the bath was monitored with a mercury thermometer that was calibrated to ½°C. The temperature for each degree change was recorded on the strip-chart by quickly blocking the reflected beam. The blocking of the beam produced a mark on the strip chart that enabled the recording of the the temperature and the fringe position at the same time interval. A circulating fan was placed inside the thermal bath to reduce the thermal gradients between the glass sample and the water bath and to increase the cooling rate.

The pressure cell employed for the hydrostatic pressure measurements is presented in Fig. 3-6. As previously stated, water was used as the compressive fluid and the measurements were conducted at room temperature. The water was transferred by the high pressure line to the pressure chamber. The glass sample was mounted on a rotatable platform at about the middle of the chamber. A 1-inch thick sapphire window provided access to the external optics. A pressure gauge used to measure the pressure level, was coupled into the pressure near the test chamber. Once optical alignment was achieved, the pressure fittings were tightened and the hydrostatic pressure was raised to about 15,000 psi. At this point a leak was introduced at the pressure coupling causing a decompression in the chamber. As in the case of the temperature measurements, the pressure and the fringe position as a function of time were recorded by quickly blocking the reflected beam.

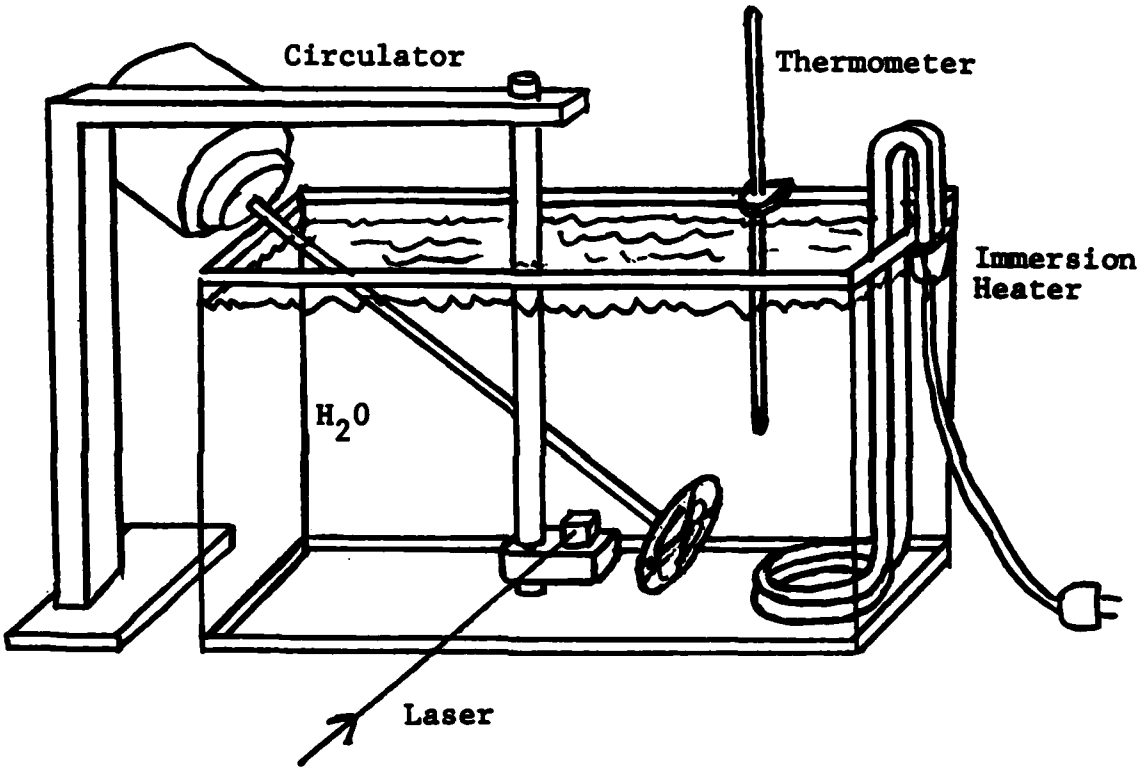

FIG. 3-5. Temperature Bath.

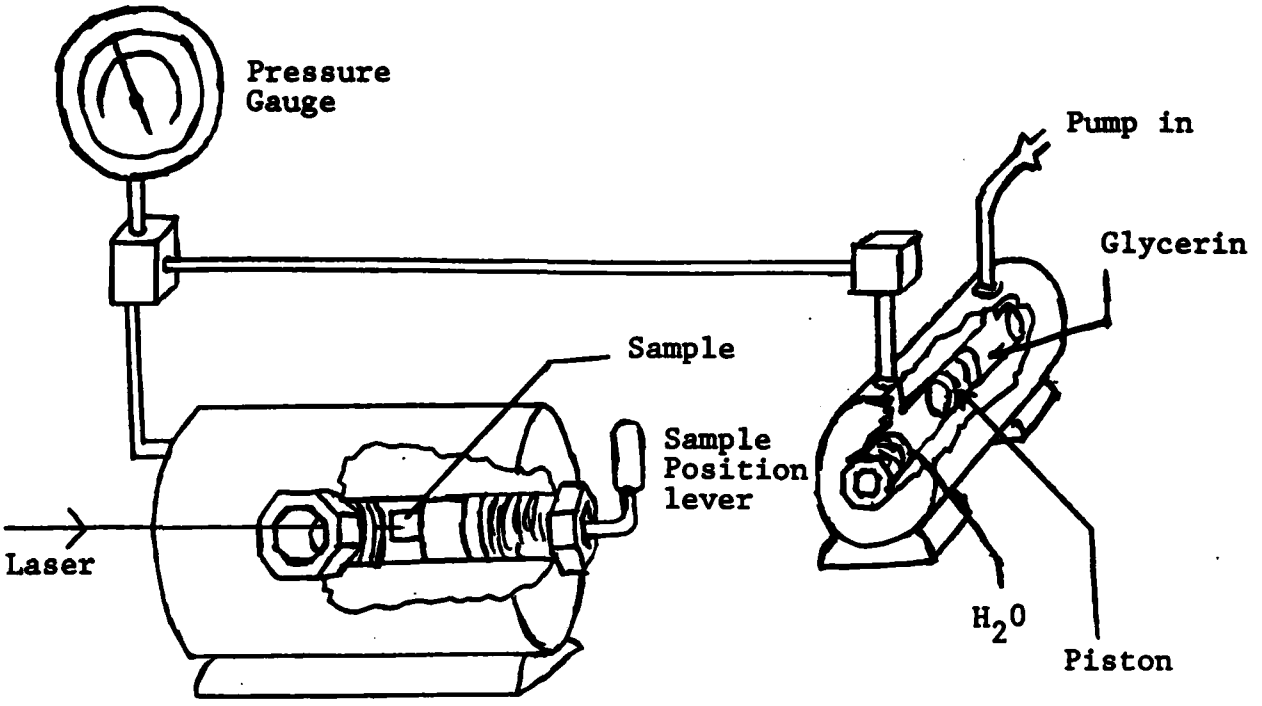

FIG. 3-6. Hydrostatic Pressure Setup.

3.3 Glass Samples

The glass samples were supplied to Tracor by Corning Glass Works, Corning, New York. The compositions and corresponding front to rear face dimensions are listed in Table 3-1. Two of the samples were fused silica; one of the silica samples had a small amount of water. The doped-silica samples were prepared using the OVPO (outside vapor phase oxidation) process. In this process, a tube of fused silica is formed and the dopant is placed within the tube. The silica is then heated and collapsed around the dopant. This causes the dopant to vaporize and infuse itself throughout the silica matrix. The samples were cut from the dowel-shaped pieces and they were ground and polished into cubes with optically flat faces. However, the infusion process produced striations in the glass samples. The striations represent significant inhomogeneities present in the doped-silica sample. These inhomogeneities are the main source of errors in the experimental results, which will be fully discussed in Section 4 of this report.

Table 3-1. List of Glass Samples and Corresponding Dopants and Dopant Concentrations.

DOPANT	LEVEL
GeO_2	5.0%
GeO_2	12.0%
GeO_2	20.0%
B_2O_3	7.0%
B_2O_3	10.0%
P_2O_5	3.0%
P_2O_5	7.0%
NONE - PURE SiO_2 - BASELINE SAMPLE	
NONE - SiO_2 + H_2O - BASELINE SAMPLE	

4.0 EXPERIMENTAL RESULTS

From the strip chart recorder traces, the fringe rates with respect to temperature ($\frac{dN_1}{dT}$ and $\frac{dN_2}{dT}$) and pressure ($\frac{dN_1}{dp}$ and $\frac{dN_2}{dp}$) were computed for all the glass samples listed in Table 3-1. In most cases, for each interferometer arrangement, four separate determinations of fringe rates were made on each sample, two separate measurements for each of the two laser wavelengths. This was done to check the repeatability of the data and reduce its experimental uncertainty. For each data set, the corresponding fringe rate was computed according to the following procedure. From the strip chart trace, the fringe order number, N_1 or N_2, and the environmental parameter, T or p, were both plotted versus time (t); the speed of the chart recorder was used as the time-base. Figure 4-1 are typical plots of fringe order number versus time and environmental parameter versus time. From plots such as these, a third plot was obtained. In this second step, time was eliminated as a variable and a plot of fringe order number versus environmental parameter was obtained. Figure 4-2 is a typical plot obtained in the second step. The experimental points from the third plot were curved fitted by the method of least squares using a North Star Horizon minicomputer system. From the slope of the best fit, the fringe rate was obtained.

For all the glass samples, the values for the fringe rates with respect to temperature and pressure are presented in Table 4-1. For each fringe rate, the table gives both its average value and the corresponding deviation. The deviation for each set of measurements has been taken to represent the experimental uncertainty in the fringe rates.

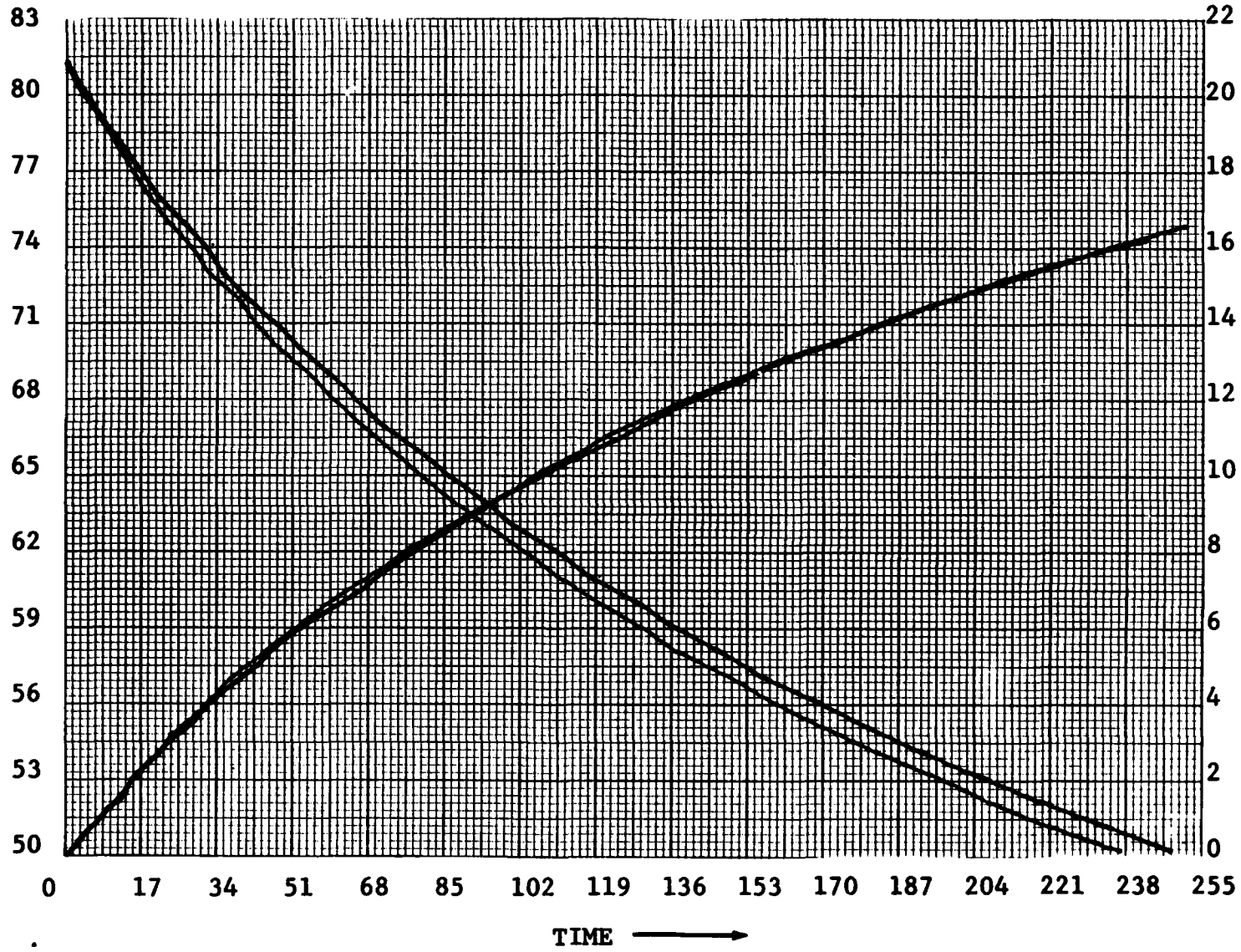

FIG. 4-1. Typical Data from Fringe Traces.

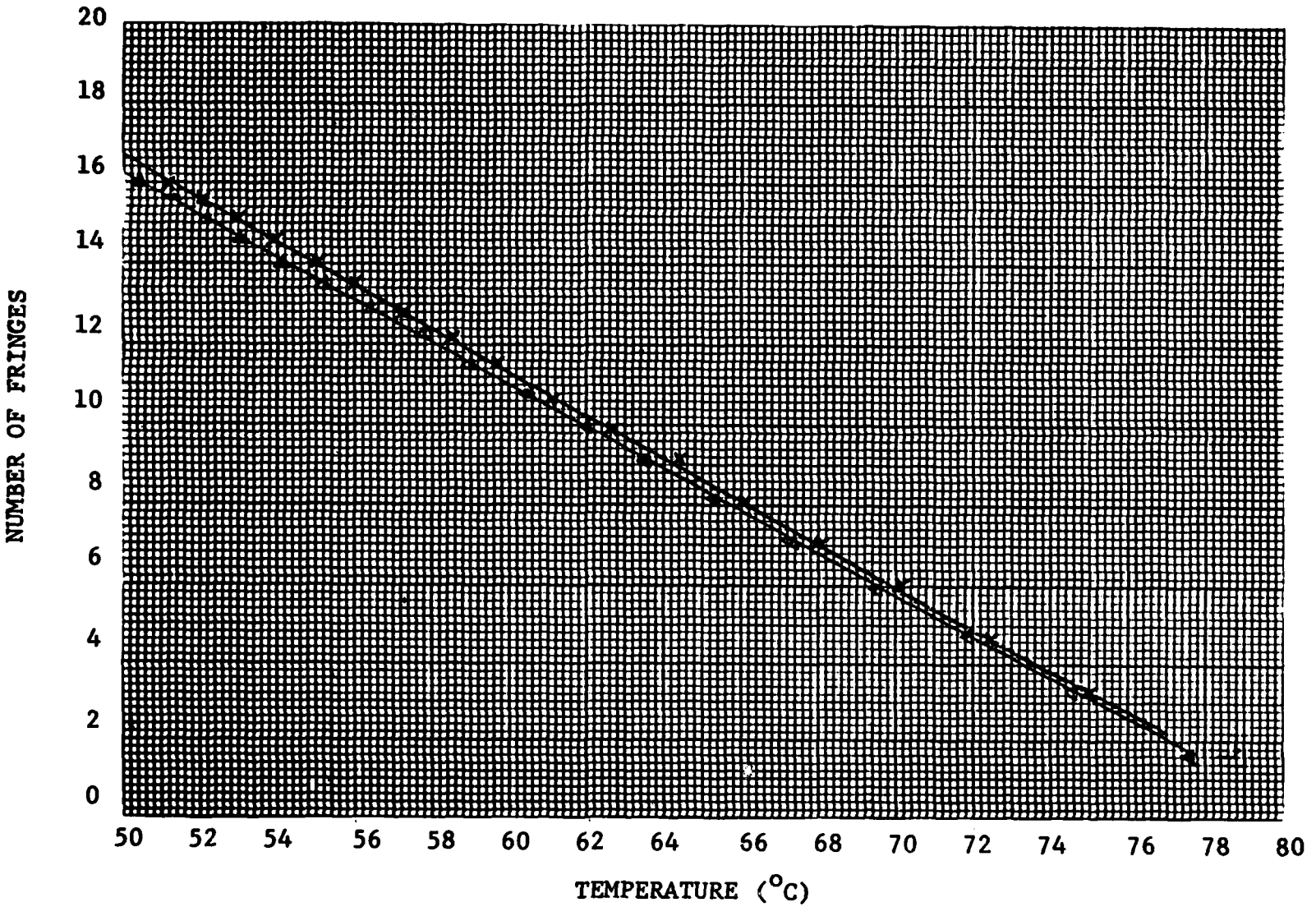

FIG. 4-2. Plots of Fringe Order Number vs. Temperature.

Table 4-1. Fringe Rate Value for all the Glass Samples.

	dN_1/dT		dN_2/dT		$dN_1/dp \times 10^3$		$dN_2/dp \times 10^3$	
	λ = 5145A	λ = 4880A	λ = 5145A	λ = 4880A	λ = 5145A	λ = 4880A	λ = 5145A	λ = 4880A
1. SiO_2	0.53	0.53	-9.05	-	-1.49	-1.62	41.32	38.61
	0.50	0.58	-8.60	-	-1.44	-1.53	40.00	-
Average Value	.54 ± 0.03		-8.83		-1.52 ± 0.07		40.0 ± 1.1	
% Deviation	6%		5%		5%		3%	
2. SiO_2+H_2O	0.52	0.55	-10.30	-	-1.62	-1.67	42.37	42.02
	0.53	0.57	-9.41	-	-1.56	-1.63	-	-
Average Value	.54 ± 0.02		-9.86		-1.62 ± 0.04		42.20	
% Deviation	4%		9%		2%		1%	
3. SiO_2+5%GeO_2	0.26	0.27	-4.56	-	-0.72	-0.78	25.58	21.79
	0.21	0.23	-4.44	-	-0.73	-0.79	-	-
Average Value	0.24 ± 0.02		-4.50		-0.76 ± 0.03		23.69	
%Deviation	8%		3%		4%		16%	
4. SiO_2+12%GeO_2	0.47	0.44	-7.42	-	-1.14	-1.20	31.85	35.59
	0.44	0.43	-7.43	-	-1.27	-1.33	-	-
Average Value	0.45 ± 0.02		-7.43		-1.22 ± 0.07		33.72	
% Deviation	4%		1%		5%		11%	
5. SiO_2+20%GeO_2	0.55	0.58	-6.45	-	-0.93	-1.85	28.57	29.50
	0.56	0.45	-6.58	-	-1.06	-1.13	-	
Average Value	0.54 ± 0.05		-6.52		-1.24 ± .36		29.04	
% Deviation	9%		2%		29%		3%	

Table 4-1. (Continued).

	dN_1/dT		dN_2/dT		$dN_1/dp \times 10^3$		$dN_2/dp \times 10^3$	
	λ = 5145A	λ = 4880A	λ = 5145A	λ = 4880A	λ = 5145A	λ = 4880A	λ = 5145A	λ = 4880A
6. SiO_2+7%B_2O_3	0.28	0.30	-6.13	-	-0.98	-1.01	27.25	26.88
	0.31	0.27	-5.99	-	-1.05	-1.14	26.60	-
Average Value	0.29 ± 0.02		-6.06		-1.05 ± 0.06		26.91 ± .27	
% Deviation	7%		2%		6%		10%	
7. SiO_2+10%B_2O_3	0.29	0.27	-	-	-0.78	-0.76	22.88	19.61
	0.22	0.22	-	-	-0.74	-0.80	-	-
Average Value	0.25 ± 0.03				-0.77 ± 0.02		21.25	
% Deviation	12%				3%		15%	
8. SiO_2+3%P_2O_5	0.30	0.32	-3.94	-	-0.69	-0.65	19.53	19.92
	0.38	-	-3.89	-	-0.60	-0.65	16.75	-
Average Value	.33 ± 0.03		-3.92		-0.65 ± 0.03		18.73 ± 1.42	
% Deviation	9%		1%		5%		8%	
9. SiO_2+7%P_2O_5	0.33	0.29	-4.88	-	-0.64	-0.65	21.41	23.04
	0.30	0.27	-4.78	-	-0.58	-0.70	-	-
Average Value	0.30 ± 0.02		-4.83		-0.64 ± 0.04		22.23	
% Deviation	7%		2%		6%		7%	

4.1 Determination of $\frac{dn}{dT}$, $\frac{dn}{dp}$, α, and k of Glass Samples Using the Optical Parameters of Water

From the fringe rates listed in Table 4-1, the values of $\frac{dn}{dT}$, $\frac{dn}{dp}$, α and k for each glass sample can be determined using the relations given in Eqs. 3-5, 3-6, 3-,7 and 3-8. However, inspection of these equations reveals that the accuracy of the experimental results depends, to a large extent, on the accurate values of the optical parameters of water. Specifically, the index of refraction of water, and its rate of change with respect to temperature and pressure, i.e., n_e, $\frac{dn_e}{dT}$ and $\frac{dn_e}{dp}$. Although the optical parameters of water have in the past been studied by several investigators, no universal agreement exists concerning their values. For example, Waxler et al. (1) give a value of $-14.5 \times 10^{-5}/^{\circ}C$ for $\frac{dn_e}{dT}$ at room temperature and at a wavelength of 5875A, while the table of values given in the AIP Handbook (2) yields a value of $-16.2 \times 10^{-5}/^{\circ}C$ at approximately the same wavelength. Similar discrepancies exist in the literature concerning the value of $\frac{dn_e}{dp}$ for water.

The experimental values of $\frac{dn}{dT}$, $\frac{dn}{dp}$, α and k for the two fused silica samples are given in Table 4-2. These values were determined from Eqs. 3-5, 3-6, 3-7, and 3-8 and the corresponding fringe rates computed from the experimental data; the index of refraction of fused silica was taken to be 1.458. This is the value measured by Schroeder (3). Table 4-2 shows that slightly different values for $\frac{dn_e}{dT}$ and $\frac{dn_e}{dp}$ for water produce large differences in the experimental results, large standard deviations, and even larger deviations from the accepted values of $\frac{dn}{dT}$, $\frac{dn}{dp}$, α and k in the literature.

Table 4-2. Values of $\frac{dn}{dT}$, α, $\frac{dn}{dp}$ and k for the Two Fused-Silica Samples Computed from Corresponding Fringe Rates for Slightly Different Values of $\frac{dn_e}{dT}$ and $\frac{dn_e}{dp}$.

Sample		$\frac{dn_e}{dT} = -14.5 \times 10^{-5}/^{\circ}C$ dn/dT ($10^{-6}/^{\circ}C$)	$\frac{dn_e}{dT} = -14.5 \times 10^{-5}/^{\circ}C$ α ($10^{-7}/^{\circ}C$)	$\frac{dn_e}{dT} = -16.2 \times 10^{-5}/^{\circ}C$ dn/dT ($10^{-6}/^{\circ}C$)	$\frac{dn_e}{dT} = -16.2 \times 10^{-5}/^{\circ}C$ α ($10^{-7}/^{\circ}C$)
1. SiO_2	Average Value	50.5 ± 15	-288.5 ± 70.4	35.1 ± 12	-165.1 ± 70.5
	% Stand Dev.	30%	24%	34%	43%
	Accepted Value	9.99	5.5	9.99	5.5
	% Deviation from Accepted Value	450%		250%	
2. SiO_2+H_2O	Average Value	46.6 ± 9.1	-397.7 ± 134.1	50.0 ± 19.4	-269.5 ± 134.1
	% Stand Dev.	20%	34%	39%	50%
	Accepted Value	9.99	5.5	9.99	5.5
	% Deviation from Accepted Value	366%		400%	

Sample		$\frac{dn_e}{dp} = 1.086 \times 10^{-6}$/psi dn/dp ($10^{-8}$/psi)	$\frac{dn_e}{dp} = 1.086 \times 10^{-6}$/psi k ($10^{-8}$/psi)	$\frac{dn_e}{dp} = 1.000 \times 10^{-6}$/psi dn/dp ($10^{-8}$/psi)	$\frac{dn_e}{dp} = 1.000 \times 10^{-6}$/psi k ($10^{-8}$/psi)
1. SiO_2	Average Value	25.5 ± 6.5	61.4 ± 22	17.6 ± 2.7	67.2 ± 28.4
	% Stand Dev.	25%	36%	15%	42%
	Accepted Value	6.27	18.84	6.27	18.84
	% Deviation from Accepted Value	306%	226%	181%	257%
2. SiO_2+H_2O	Average Value	31.7 ± 5.5	58.8 ± 12.6	20.1 ± 5.5	39.1 ± 11.3
	% Stand Dev.	17%	21%	27%	29%
	Accepted Value	6.27	18.84	6.27	18.84
	% Deviation from Accepted Value	406%	212%	221%	108%

In fact as it may be noted, although the maximum standard deviation in the corresponding fringe rates was only 10%; the maximum standard deviation in the experimental results with respect to the accepted values was more than 400%. The underlying reason for these large experimental errors in the values of $\frac{dn}{dT}$, $\frac{dn}{dp}$, α, and k, lies in the fact that their values are determined from differences in quantities that are very close to each other. For example, $\frac{dn}{dT}$ (Eq. 4-5) was determined by the difference between $\frac{n}{n_e}\frac{dn_e}{dT}$ and $\frac{\lambda}{2t}\left(\frac{dN_1}{dT} - \frac{n}{n_e}\frac{dN_2}{dT}\right)$.

This is because the first term in the equation is negative, while the second term is positive. This means that small experimental uncertainties in the values of n_e, $\frac{dn_e}{dT}$, $\frac{dn_e}{dp}$, etc. can greatly magnify the experimental uncertainty in the experimental values of $\frac{dn}{dT}$, $\frac{dn}{dp}$, α and k for the glass sample. Consequently, the experimental error in the fringe rates and the uncertainty in the rate of change in the index of refraction of water must be extremely small, if the present interferometric method were to have yielded meaningful results. This appears to be impossible in view of the fact that significant inconsistencies exist in the literature concerning the "accepted" values of $\frac{dn_e}{dT}$ and $\frac{dn_e}{dp}$ for water. Although not reported for the sake of brevity, the value of $\frac{dn}{dT}$, α, $\frac{dn}{dp}$ and k of the doped-silica samples when computed from Eqs. 3-5, 3-6, 3-7, and 3-8 had large experimental errors.

4.2 Determination of $\frac{dn}{dT}$ and $\frac{dn}{dp}$ of Glass Samples Without Using the Optical Parameters of Water

The values of $\frac{dn}{dT}$ and $\frac{dn}{dp}$ for the glass samples may be computed using only part of the experimental data, namely, the data associated with the

fringe rates $\frac{dN_1}{dT}$ and $\frac{dN_1}{dp}$, resulting from optical path differences due to changes, both in the index of refractions and in the dimensions of the glass samples. When this is done, $\frac{dn}{dT}$ and $\frac{dn}{dp}$ may be determined through the following expressions:

$$\frac{dn}{dT} = \frac{\lambda}{2t}\frac{dN_1}{dT} - n\alpha \qquad (4\text{-}1)$$

$$\frac{dn}{dp} = -\frac{\lambda}{2t}\frac{dN_1}{dp} + \frac{kn}{3} \qquad (4\text{-}2)$$

As shown by the above two expressions, $\frac{dn_e}{dT}$ and $\frac{dn_e}{dp}$ of water do not enter into the calculations. However, the values of the expansion coefficient, α, the compressibility, k, and the index of refraction, n, of the glass samples must be independently known in order to determine $\frac{dn}{dT}$ and $\frac{dn}{dp}$. Fortunately, the values of α, k, and, n for the different dopants and dopant concentrations present in the doped-silica samples have been measured by Dr. George Scherer at Corning Laboratory (4). Table 4-3 is a summary of the values provided by Scherer; the values of α and k for the fused-silica samples were taken from the references given in the table. The compressibility values for the phosphate dopant were not available. Therefore, $\frac{dn}{dp}$ for the phosphate-doped sample could not be computed. Tables 4-4 and 4-5 summarize the experimental values of $\frac{dn}{dT}$ and $\frac{dn}{dp}$ computed from Eqs. 4-1 and 4-2, and the corresponding values of n, α, and k given in Table 4-3. As it may be noted from Tables 4-4 and 4-5, the maximum standard deviation for the doped silica samples was about 13% for $\frac{dn}{dT}$ and about 6% for $\frac{dn}{dp}$. The standard deviations, in most cases, were based on four separate experimental values of $\frac{dn}{dT}$ and $\frac{dn}{dp}$ for each glass sample. The values of $\frac{dn}{dT}$ and $\frac{dn}{dp}$ for the fused-silica samples fell within 2-4% of the accepted literature values (5, 6, 7, 8).

Table 4-3. Values of Index of Refraction, n, Coefficient of Thermal Expansion, α, and Compressibility, k, of Glass Samples as Functions of Dopant and Dopant Concentration.

SAMPLE	INDEX OF REFRACTION[a] n (λ = 5893A)	THERMAL EXPANSION[b] COEFFICIENT $x10^{7}/^{o}C$	COMPRESSIBILITY[c] $k/3 \times 10^{8}$/psi
1. SiO_2	1.458	5.5	6.28±0.10
2. SiO_2+H_2O	1.458	5.5	6.28±0.10
3. SiO_2+5%GeO_2	1.4599±2x10^{-4}	7.4±1	6.07±0.20
4. SiO_2+12%GeO_2	1.4605±2x10^{-4}	12.6±1	6.26±0.20
5. SiO_2+20%GeO_2	1.4750±2x10^{-4}	18.2±1	6.50±0.20
6. SiO_2+7%B_2O_3	1.4565±2x10^{-4}	10.3±1	6.66±0.20
7. SiO_2+10%B_2O_3	1.4561±2x10^{-4}	12.3±1	6.91±0.20
8. SiO_2+3%P_2O_5	1.4595±2x10^{-4}	6.9±1	
9. SiO_2+7%P_2O_5	1.4617±2x10^{-4}	9.4±1	

a) Index of refraction measured by Backeline technique

b) Coefficient of thermal expansion measured with fused silica dilatometer

c) Young's modulus measurements by an ultrasonic method

$\frac{k}{3} = (1-2\sigma)/E$, E = Young's modulus, σ = Poisson's ratio

σ = 0.2 for the doped glass samples

Table 4-4. Values of $\frac{dn}{dT}$ of the Glass Samples Computed from Equation 4-1.

	SAMPLE	$\frac{dn}{dT} \times 10^6/^oC$		ACCEPTED VALUE
1.	SiO_2	514	10.33	
		514	9.71	
		488	9.61	
		488	10.60	
		average value	10.06±0.40	$9.99 \times 10^{-6}/^oC$ for λ = 5893A[a]
		percent deviation	4(<1%)	
2.	SiO_2+H_2O	514	9.71	
		514	9.89	
		488	9.60	
		488	10.15	
		average value	9.84±0.14	
		percent deviation	1.4	
3.	SiO_2+5% GeO_2	514	9.88	
		514	7.91	
		488	9.84	
		488	8.22	
		average value	8.96±0.83	
		percent deviation	9.2	
4.	SiO_2+12% GeO_2	514	9.42	
		514	10.34	
		488	8.98	
		488	8.74	
		average value	9.37±0.52	
		percent deviation	5.6	
5.	SiO_2+20% GeO_2	514	13.64	
		514	13.86	
		488	13.74	
		488	9.96	
		average value	12.8±0.82	
		percent deviation	12.8	

Table 4-4 (Continued).

SAMPLE	$\frac{dn}{dT} \times 10^6/°C$	ACCEPTED VALUE
6. SiO_2+17% B_2O_3	514	7.58
	514	8.38
	488	7.46
	488	6.62
	average value	7.50±0.43
	percent deviation	5.8
7. SiO_2+10% B_2O_3	514	9.20
	514	6.64
	488	7.77
	488	6.08
	average value	7.12±0.99
	percent deviation	13.4
8. SiO_2+3% P_2O_5	514	13.12
	514	16.88
	488	12.18
	488	11.10
	average value	13.5±1.74
	percent deviation	12.9
9. SiO_2+7% P_2O_5	514	11.26
	514	10.20
	488	-
	average value	10.57±0.49
	percent deviation	4.6

(a) Corning Laboratory, Corning, NY

Table 4-5. Values of $\frac{dn}{dp}$ of the Glass Samples Computed from Equation 4-2.

SAMPLE	$\frac{dn}{dp} \times 10^{8}$/psi		ACCEPTED VALUES	
1. SiO_2	514	6.06		
	514	6.16		
	488	5.95		
	488	6.15	for λ = 5893A	$6.34 \pm 0.25 \times 10^{-8}$/psi [a]
	average value	6.08 ± 0.08	for λ = 5875A	$5.96 \pm 0.14 \times 10^{-8}$/psi [b]
	percent deviation	1.3(2-4%)	for λ = 5893A	6.27×10^{-8}/psi [c]
2. SiO_2+H_2O	514	5.91		
	514	6.04		
	488	6.07		
	488	5.99		
	average value	6.00 ± 0.06		
	percent deviation	1 (2-4%)		
3. SiO_2+5% GeO_2	514	5.71		
	514	5.77		
	488	5.67		
	488	5.64		
	average value	5.70 ± 0.05		
	percent deviation	0.9		
4. SiO_2+12% GeO_2	514	6.16		
	514	5.82		
	488	6.15		
	488	5.84		
	average value	5.99 ± 0.16		
	percent deviation	2.7		
5. SiO_2+20% GeO_2	514	6.82		
	514	6.42		
	488	6.20		
	488	-		
	average value	$6.48 \pm .29$		
	percent deviation	4		

Table 4-5 (Continued).

SAMPLE	$\frac{dn}{dp} \times 10^6$/psi	ACCEPTED VALUES
6. SiO_2+B_2O_3 7%	514	6.57
	514	6.35
	488	6.62
	488	6.25
	average value	6.45±0.15
	percent deviation	2.4
7. SiO_2+10% B_2O_3	514	7.14
	514	7.29
	488	7.35
	488	7.20
	average value	7.26±0.08
	percent deviation	1

[a] K. Vedam, E.D.D. Schmidt, and Rustum Roy, "Non-linear Variation of Refractive Index of Vitreous Silica with Pressure to 7 kbars", Journal of the American Ceramic Society, Vol. 49, No. 10, 1966.

[b] R. M. Waxler and C. E. Weir, "Effect of Hydrostatic Pressure on Refractive Indices of Some Solids", Journal of Research of NBS-A. Physics and Chemistry, Vol. 69A, No. 4 July-August 1965.

[c] R. Bruckner, "Properties and Structure of Vitreous Silica I", Journal of Non-Crystalline Solids 5 (1970), 123-175.

4.2.1 Large Inhomogeneities in Doped-Silica Glasses Limit Accuracy of Experimental Results. When the optical parameters of water were not used to determine the values of $\frac{dn}{dT}$ and $\frac{dn}{dp}$, most of the experimental errors have been traced to the non-uniform distribution of the dopandants within the glass samples. This is consistent with the fact that results on the pure silica samples had smaller experimental errors than the doped-silica samples. Thus, the non-uniform distribution of the dopants gave rise to large inhomogeneities in the glass samples. These inhomogeneities, in turn, led to large experimental deviations in the values of $\frac{dn}{dT}$ and $\frac{dn}{dp}$. Since one of the basic objectives of the optical measurements was to study the effect of dopant and dopant concentration on the rate of change of the index of refraction with respect to temperture and pressure, the presence of large inhomogeneities in the glass samples limited the accuracy of the results and, consequently their usefulness. This fact together with the problems encountered with optical parameters of water, suggest the need to conduct the optical measurements on better quality glass samples, using experimental techniques that do not involve water.

5.0 CONCLUSIONS AND RECOMMENDATIONS

Laser interferometry was employed to determine the rate of change of the index of refraction with respect to temperature and pressure, the expansion coefficient and the compressibility of doped-silica glass samples for three types of dopants and different dopant concentration for a given dopant. Two fused silica samples were also included in the optical measurements to check the validity of the experimental method and to establish baseline values for the quantities being measured. Water was used as thermal bath for the temperature measurements and as the compressive fluid for the pressure measurements. The significant observations from the present investigation are summarized as follows:

(1) When the optical parameters of water, $\frac{dn_e}{dT}$, $\frac{dn_e}{dp}$ and n_e, were used to determine the elasto-optic properties of the doped-silica samples, the resulting experimental errors were quite large. The large errors were partly due to significant inconsistencies existing in the literature concerning the value of $\frac{dn_e}{dT}$ and $\frac{dn_e}{dp}$ for water, and partly due to the fact that the experimental method computed the elasto-optic properties from differences in quantities that were very close to each other. These two factors greatly magnified the experimental errors.

(2) A way was found to compute the elasto-optic quantities from only part of the experimental data; the data that did not involve the parameters of water. When this was done, the maximum experimental deviation for the doped-silca samples was about 13% for $\frac{dn}{dT}$ and about 6% for $\frac{dn}{dp}$; the values of $\frac{dn}{dT}$ and $\frac{dn}{dp}$ for the two pure silica samples were within few percent of the literature values.

(3) When the water parameters did not enter in determination of $\frac{dn}{dT}$ and $\frac{dn}{dp}$, most of the remaining experimental uncertainty was traced to the large inhomogeneities present in the doped-silica samples. These inhomogeneities greatly limited the usefulness of the experimental results.

In view of the above conclusions, it is recommended that the optical measurements be carried out on better quality glass samples using experimental techniques that do not involve water and where the specific quantities to be measured are not computed from difference of quantities that are too close to each other. The above recommendations have been discussed in a proposal that Tracor presented to ONR (9). The proposal is currently being reviewed by Dr. Pohanka at ONR and by Dr. Bucaro's group at NRL.

REFERENCES

1. Waxler, R. M., C. E. Weir, and H. W. Schamp, Jr. "Effects of Pressure and Temperature upon the Optical Dispersion of Benzene, Carbon Tetrachloride and Water," J.R.N. Bur. Stand. Sec. A., 68A, No. 5 (Sept. - Oct. 1964), 489-497.

2. Weast, Robert C., ed. Handbook of Chemistry and Physics, 45th ed., Ohio: 1964-65, E 105.

3. Schroeder, John, "Brillouin Scattering and Pockels Coefficients in Silicate Glasses," Accepted for Publication in J. Non-Cryst. Solids - Aug. 1979.

4. Private communication with Dr. George Sherer.

5. Waxler, R. M. and G. W. Cleek, "Refractive Indices of Fused Silica at Low Temperature," J.R.N. Bur. Stand. Sec. A, 75A, No. 4 (July - Aug. 1971), 279-281.

6. Vedom, K., E. D. D. Schmidt, and Rustum Roy, "Non-linear Variation of Refractive Index of Vitreous Silica with Pressure to 7K bars", Journal of the American Ceramic Society, Vol. 49, No. 10, 1966.

7. Waxler, R. M., and C. E. Weir, "Effect of Hydrostatic Pressure on Refractive Indices of Some Solids," Journal of Research of NBS-A Physics and Chemistry, Vol. 69A, No. 4 (July - Aug. 1965).

8. Bruckner, R., "Properties and Structure of Vitreous Silica I," Journal of Non-Crystalline Solids, No. 5, (1970) 123-175.

9. "Experimental Measurements of Optical Fiber Materials by Interferometric and Brillouin Scattering Techniques", Tracor proposal to ONR, 22 July 1980.